REPORT DOCUMENTATION PAGE

Form Approved OMB NO. 0704-0188

1. REPORT DATE (DD-MM-YYYY)	2. REPORT TYPE	3. DATES COVERED (From - To)
	New Reprint	-

4. TITLE AND SUBTITLE	5a. CONTRACT NUMBER
Operating modes and power considerations of microhollow cathode discharge devices with elongated trenches	W911NF-07-1-0118
	5b. GRANT NUMBER
	5c. PROGRAM ELEMENT NUMBER
	611102

6. AUTHORS	5d. PROJECT NUMBER
E.A. Lennon, A.A. Burke, R.S. Besser	
	5e. TASK NUMBER
	5f. WORK UNIT NUMBER

7. PERFORMING ORGANIZATION NAMES AND ADDRESSES	8. PERFORMING ORGANIZATION REPORT NUMBER
Stevens Institute of Technology Stevens Institute of Technology Castle Point on Hudson Hoboken, NJ 07030 -	

9. SPONSORING/MONITORING AGENCY NAME(S) AND ADDRESS(ES)	10. SPONSOR/MONITOR'S ACRONYM(S)
U.S. Army Research Office P.O. Box 12211 Research Triangle Park, NC 27709-2211	ARO
	11. SPONSOR/MONITOR'S REPORT NUMBER(S)
	51422-CH.3

12. DISTRIBUTION AVAILIBILITY STATEMENT

Approved for public release; distribution is unlimited.

13. SUPPLEMENTARY NOTES

The views, opinions and/or findings contained in this report are those of the author(s) and should not contrued as an official Department of the Army position, policy or decision, unless so designated by other documentation.

14. ABSTRACT

Microhollow cathode discharge (MHCD) devices generate microplasmas with high electron densities and reactive species, making them a prospective hydrocarbon reforming technology. Here we report on the electrical phenomena resulting from MHCD devices with elongated trenches using argon at atmospheric pressure and room temperature. Devices that were 100 mm wide, 100 mm deep, and 1 cm long exhibited self-pulsing current during constant voltage DC power application ranging from 0 mA to 32 mA. The

15. SUBJECT TERMS

Microplasma, Nonthermal plasma, Microhollow cathode discharge, Self-pulsing, Hydrocarbon reforming, Fuel cell

16. SECURITY CLASSIFICATION OF:			17. LIMITATION OF ABSTRACT	15. NUMBER OF PAGES	19a. NAME OF RESPONSIBLE PERSON
a. REPORT	b. ABSTRACT	c. THIS PAGE	UU		Ronald Besser
UU	UU	UU			19b. TELEPHONE NUMBER
					201-216-5257

Report Title

Operating modes and power considerations of microhollow cathode discharge devices with elongated trenches

ABSTRACT

Microhollow cathode discharge (MHCD) devices generate microplasmas with high electron densities and reactive species, making them a prospective hydrocarbon reforming technology. Here we report on the electrical phenomena resulting from MHCD devices with elongated trenches using argon at atmospheric pressure and room temperature. Devices that were 100 mm wide, 100 mm deep, and 1 cm long exhibited self-pulsing current during constant voltage DC power application ranging from 0 mA to 32 mA. The capacitances for MHCDs with trenches 25, 100, and 250 mm wide were estimated to be 68, 70, and 33 mF respectively. A current-limited DC supply prevented self-pulsing, and resulted in abnormal, normal, or negative differential resistance (NDR), i.e. hollow cathode, operating modes. The NDR state manifested at lower current limits and occurred when the microplasma in the trench was discontinuous. Simulations from a corresponding, empirically determined circuit model showed larger total average power consumption (including the ballast resistance) during pulsed inputs (5.61e31.08 W) in comparison to constant voltage inputs (<1 W). These ?ndings advance the development of these MHCDs for microplasma reforming applications, providing insights into operational modes and power consumption estimates critical to understanding the overall ef?ciency in the context of a future microplasma reforming system.

REPORT DOCUMENTATION PAGE (SF298)
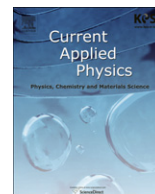## (Continuation Sheet)

Continuation for Block 13

ARO Report Number   51422.3-CH
Operating modes and power considerations of m   ...

Block 13: Supplementary Note

Operating modes and power considerations of microhollow cathode discharge devices with elongated trenches

E.A. Lennon [a],[*], A.A. Burke [b], R.S. Besser [a]

[a] Department of Chemical Engineering and Materials Science, Stevens Institute of Technology, Castle Point on Hudson, Hoboken, NJ 07030, United States
[b] Naval Undersea Warfare Center, 1176 Howell Street, Newport, RI 02841, United States

ABSTRACT

Microhollow cathode discharge (MHCD) devices generate microplasmas with high electron densities and reactive species, making them a prospective hydrocarbon reforming technology. Here we report on the electrical phenomena resulting from MHCD devices with elongated trenches using argon at atmospheric pressure and room temperature. Devices that were 100 μm wide, 100 μm deep, and 1 cm long exhibited self-pulsing current during constant voltage DC power application ranging from 0 mA to 32 mA. The capacitances for MHCDs with trenches 25, 100, and 250 μm wide were estimated to be 68, 70, and 33 μF respectively. A current-limited DC supply prevented self-pulsing, and resulted in abnormal, normal, or negative differential resistance (NDR), i.e. hollow cathode, operating modes. The NDR state manifested at lower current limits and occurred when the microplasma in the trench was discontinuous. Simulations from a corresponding, empirically determined circuit model showed larger total average power consumption (including the ballast resistance) during pulsed inputs (5.61−31.08 W) in comparison to constant voltage inputs (<1 W). These findings advance the development of these MHCDs for microplasma reforming applications, providing insights into operational modes and power consumption estimates critical to understanding the overall efficiency in the context of a future microplasma reforming system.

1. Introduction

Over the last decade microplasma attributes, such as operability near or at atmospheric pressure and low temperature, and high electron density (experimentally determined between 10^{14} cm^{-3} and 10^{16} cm^{-3} with argon [1−5]) sparked the expansion of microplasma research into a wide-breadth of applications including those in chemical [6−12], biomedical [5,13−18], and aerospace engineering fields [4,19]. This study describes and characterizes observed electrical phenomena of microhollow cathode discharge (MHCD) devices with elongated trenches capable of sustaining microplasmas (Fig. 1). The reported MHCD devices' operating modes and power consumption were considered within the specific context of the MHCDs' potential application as a microplasma reforming device for conversion of hydrocarbons integrated with portable fuel cell power systems requiring hydrogen or synthesis gas feeds.

The MHCD has been one of the most readily fabricated and investigated microplasma devices over the last decade [3,4,6,11,20−24]. While the term "hollow cathode" historically refers to a plasma device that physically has a hollow or open space in the cathode and exhibits a negative differential resistance (NDR) operating mode, i.e. voltage drop with increasing current [5,25], investigators have also reported that MHCDs exhibit voltage and current characteristics indicative of the Townsend, normal, and abnormal glow regimes [3−5,20,22,23,25−38]. In the normal glow regime, voltage remains steady as current increases, whereas in the abnormal glow regime, voltage increases with current [5,26]. Schoenbach et al. were the first to demonstrate near atmospheric pressure (350 torr) operation of a microplasma device using a cylindrically shaped MHCD (Fig. 1) [20]. Other groups have used Schoenbach et al.'s simple device design, which consisted of a dielectric material, like mica, separating two metal electrodes with a sub-millimeter diameter hole for the gas, as a basis for other MHCD device designs [3,4,6,21,23,26−29]. For example, Chen et al. micro-machined silicon-based MHCD arrays to test various designs, one of which was a vertical cavity etched into a silicon cathode using deep reactive ion etching (Fig. 1) [23]. Since the name microhollow cathode discharge can be a source of confusion, other

* Corresponding author. Tel.: +1 201 216 5523.
E-mail addresses: elennon@stevens.edu (E.A. Lennon), adrian.burke@navy.mil (A.A. Burke), rbesser@stevens.edu (R.S. Besser).
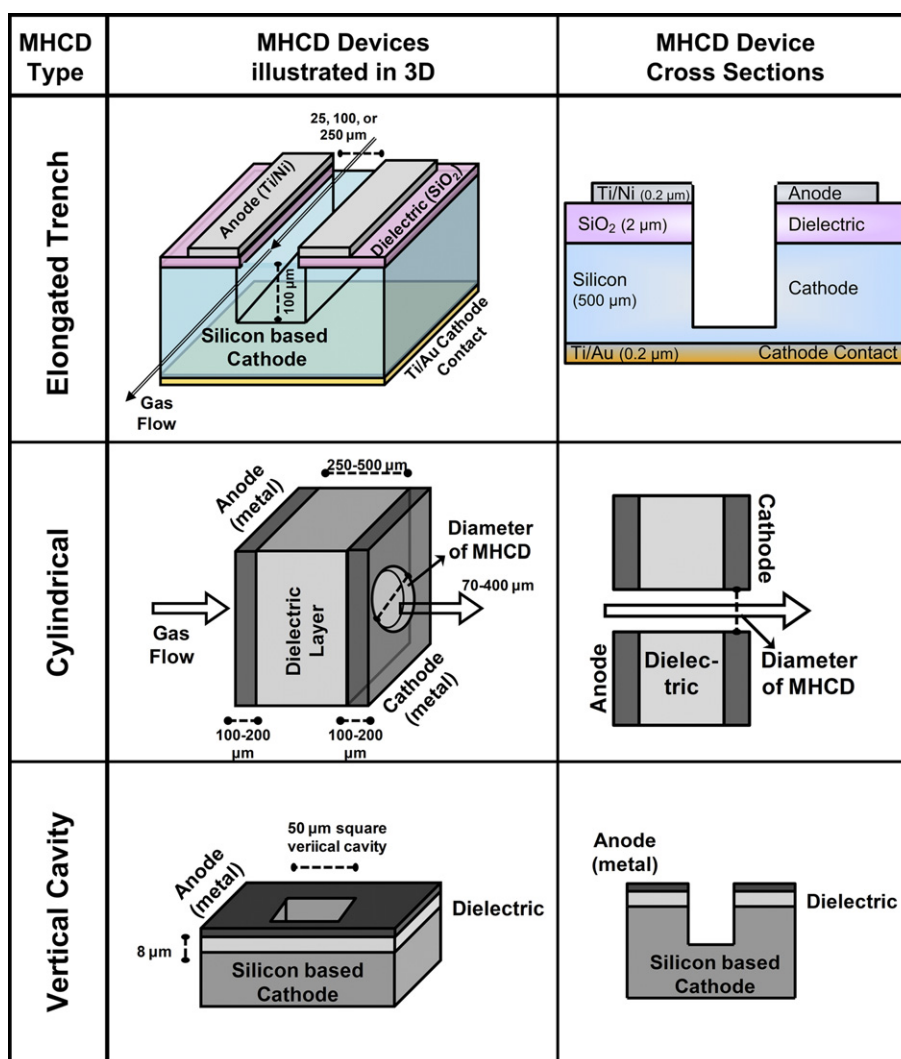
Fig. 1. Three dimensional and cross sectional views with stated dimensions of the design of the microhollow cathode discharge (MHCD) device with an elongated trench and analogous views for a cylindrical and vertical cavity MHCD [20,23].

groups may refer to such devices more generally as micro-discharges [5]. Throughout this paper the original term micro-hollow cathode discharge will be used, particularly given the fact that its physical geometry is based on a hollow cathode and the devices investigated and described more completely in later sections exhibited NDR.

The ability of MHCDs to operate in various modes means there are transitions between modes that can lead to unstable states which can manifest as self-pulsing of the voltage, current, and optical emissions [24–35,39–42]. These instabilities present a key challenge that must be addressed in order to implement MHCD devices as microreactors in which steady product streams are not only desirable, but often essential. Self-pulsing MHCDs have been observed and simulated during DC power application with various geometries [26,35,39–42], and we report on similar observed phenomena for the new devices investigated in this study. Although self-pulsing responses during DC power application is indicative of operating instability, the exceptionally high electron density produced within MHCDs remains a large impetus for exploring them as chemical reactors [1,3,5,43,44]. Increased understanding of the conditions that ensure stable microplasma operation is critical to enabling the use of the reported MHCD

devices with elongated trenches in chemical conversion applications. For the specific application of hydrocarbon reforming, it is also critical to understand the power consumption during stable operation and with alternate types of input power, such as pulsed DC. The device characterization and associated circuit model presented in this work advance both of these aspects toward the development of these MHCDs for microplasma reforming applications.

2. Experimental details

2.1. Microhollow cathode discharge (MHCD) devices with elongated trenches

Fig. 1 one depicts the three dimensional and cross sectional views of the microhollow cathode discharge (MHCD) design with an elongated trench, as well as examples of earlier MHCD designs [20,23].

The design of an elongated-trench MHCD for reforming capitalizes on the benefits of general microchannel reactors, such as large surface to volume ratio and resulting enhanced heat and mass transport, which can facilitate chemical conversion [45–47]. The

flow-through operability of the cylindrical MHCD and the ability to fabricate the vertical cavity MHCD using microelectronic fabrication (Fig. 1), were both design aspects incorporated into the elongated trench devices. The elongated trench was conceptually based on earlier microchannel reactors [45–47], and also bears a resemblance to a micro-slit device first introduced by Zhu et al. [34], but the devices in this study are made from silicon wafers using micromachining processes yielding the advantage of standardized device production. In our geometry the trench is perpendicular to the axis between the anode and cathode. The illustrated design featuring the elongated trench also extends the microplasma reactive environment for chemical conversion.

To fabricate the elongated-trench MHCD devices, a silicon dioxide (SiO_2) layer of either 2 µm, which constitutes the dielectric layer, was grown on top of highly doped silicon wafers 100 mm in diameter using high temperature oxidation. Lift-off lithography and nickel deposition including a titanium adhesion layer followed to form the Ni/Ti electrode contacts. To create the rectangular trenches in the silicon cathode deep reactive ion etching was used. A thin layer of titanium/gold (Ti/Au) was evaporated onto the back side of the wafer as a low resistance cathode contact [11]. Fig. 1 further identifies the materials used for each layer of the MHCD and details pertinent dimensions. Specifically, the depth of the trench was 100 µm and the width was 25, 100, or 250 µm. The lengths of the device and inner trench were 1 cm. Fig. 2 shows one of the fabricated device chips atop a US one cent coin for visual reference.

2.2. MHCD device holder for flow-through microplasma operation

A gas-tight MHCD device chamber, referred to as the chip holder, which had electrical contacts and gas inlet and outlet connections, was machined from Lexan™ in order to facilitate the flow of gases through the microplasma environment. The space volume in the chip holder was 1 cm³. This volume is not optimal for chemical conversion studies, since it permits reactants to bypass the plasma; however, it is adequate for studies of inert plasmas as reported here. Fig. 3 is an image of the chip holder with labels indicating the locations of the electrical connections, gas hookups, and the materials of construction.

2.3. Experimental setup

The operating modes and stability characteristics of our elongated-trench devices were investigated using the experimental setup shown in Fig. 4 with argon gas.
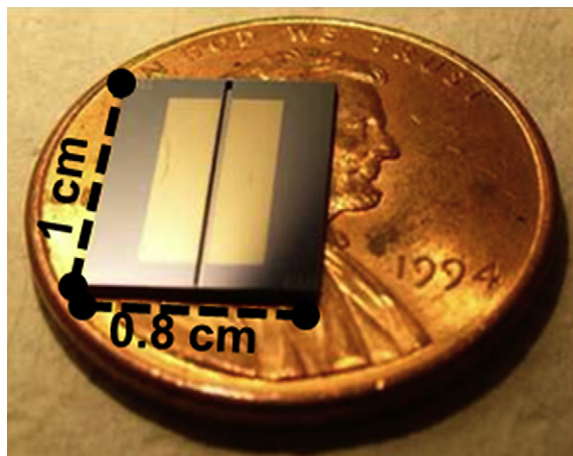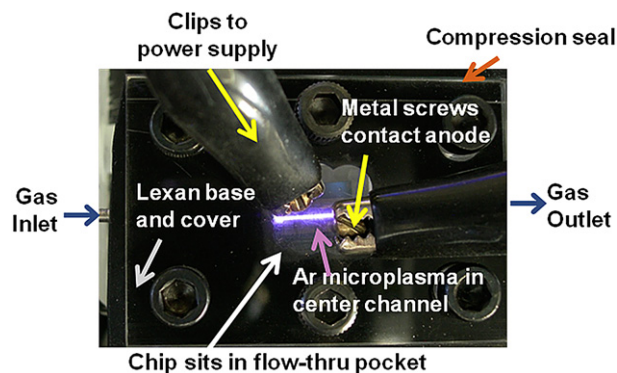

Fig. 3. Image of the microplasma chip holder made of Lexan™ during operation of MHCD chip with Ar. Alligator clips connected to the metal screws contacting the MHCD anode and cathode. One sixteenth inch-inner diameter stainless steel tubing was used for the gas inlet and outlet.

Research grade Ar flowed from the gas tank through the regulator to a mass flow controller (MFC) (Aalborg, Inc). The Ar flow rate was 7.3 standard cm³/min for all reported experiments. The Ar continued through the chip holder inlet into the MHCD, where the plasma was sustained, and then exited through the chip holder outlet. The chip holder was able to freely exchange heat with the ambient environment. Any heating effects were from electrical energy input into the MHCD devices. The inside of the chip holder, where the MHCD device sat, was at atmospheric pressure. The gas stream leaving the device under test proceeded to a Quadrupole Mass Spectrometer (QMS) and exited to the atmosphere via the QMS out vent.

Either a high constant voltage DC power supply without current-limiting capability (Hewlett–Packard) or a high voltage, current-limited DC power supply (Stanford Research Systems, Inc.) was used to apply DC power to the MHCD device under test. A series resistive network with an equivalent resistance ranging from 2.2 kOhm to 4.1 kOhm served as a small ballast resistor (R_b). The anode connected to the ballast resistor which connected to the high voltage power supply as shown in Fig. 4. The cathode connected to a screw on the underside of the chip holder, which in turn connected to ground. An oscilloscope (Tektronix 2014B) transmitted the MHCD voltage and total current data from the respective high voltage (V_m) and current probes (I_m) to the computer via a USB connection. The Tektronix P5100 high voltage probe and the Tektronix TCP312 current probe in combination with the Tektronix

Fig. 2. Photo of a fabricated MHCD device 1.00 cm long and 0.80 cm wide on top of a US one cent coin.
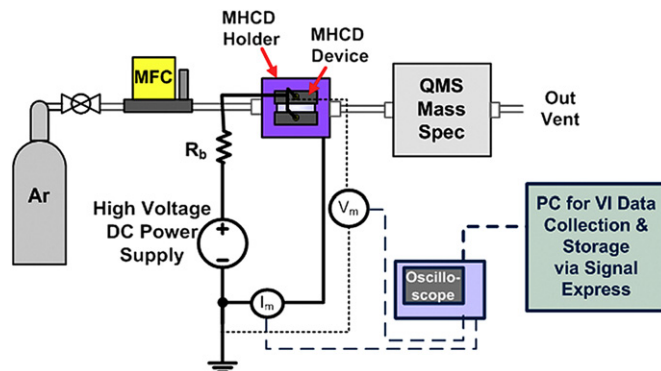

Fig. 4. Schematic of experimental setup. Tubing denotes fluidic connections, heavy lines denote electrical connections including those with the high voltage power supply, and dashed lines denote the measured voltage (V_m) and current (I_m) data viewable on the oscilloscope and stored on the PC.

TCPA300 current signal amplifier were used during the data collection. The computer recorded the VI data using Signal Express™ Software.

3. Circuit model for the MHCD device during normal mode

Various electric circuit models capturing MHCD self-pulsing current and voltage behaviors have been developed [26,39,41,42]. The schematic depicted in Fig. 5 shows the electric circuit developed to simulate the discharge voltage ("V" in Fig. 5), current ("I"), and the total current ("$I_t = I_1 + I$") during stable modes of operation, such as the normal mode, with DC or pulsed-DC input voltages. The circuit model proposed by Chabert et al. for a cylindrical MHCD provided the basis of the MHCD circuit model developed in this study [42]. The elements enclosed within the dashed lines are the components representative of the MHCD and include a microplasma capacitance ("C") in parallel with a microplasma resistance ("R_p"), and inductance ("L_p") [26,39–42]. Although the microplasma inductance "L_p" was found to be quite small, and according to the earlier findings exhibits little impact on the voltage and current dynamics during DC power application [42], we included the small microplasma inductance for the sake of model completeness. Including the microplasma inductance also enables a more robust starting point for future investigations of response dynamics with other types of power sources, such as high frequency pulsed power application, in which case the effect of microplasma inductance could play a greater role.

The MHCD circuit model in Fig. 5 uses values we empirically determined for the stable mode microplasma resistance ("R_p (Stable Mode)") and capacitance from our devices. For our simplified, limited model R_p is set to the resistance value that was observed during a normal, stable mode of operation. In particular, the plasma resistance determined during stable mode operation for the 25 μm wide device was estimated using the general expression, $R_p = \langle V_{stable} \rangle / \langle I_{stable} \rangle$, in which the brackets signify the average stable current and voltage over the full duration of stable operation. The calculated value for R_p was 88 kOhm, but was rounded to 100 kOhm in the model. Using that fixed plasma resistance value ensured the simulation of the stable operating mode specific to our MHCD device, in which a steady discharge current and voltage resulted from DC power application. It was assumed that a stable mode of operation was a preferred operating state for the elongated-trench MHCD devices in chemical conversion applications, like fuel reforming.
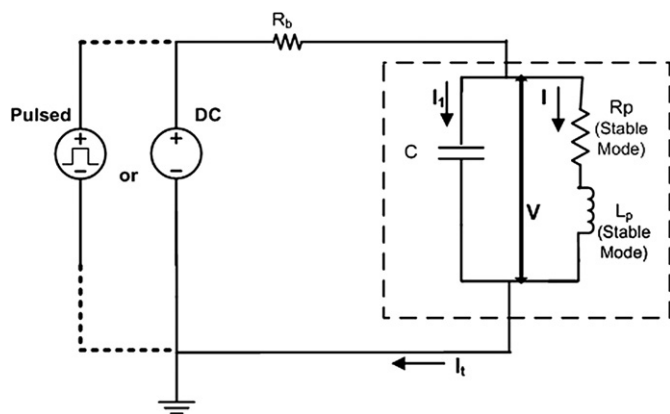
Limiting the simulation model to the stable mode of operation provided a basis for direct comparison of the MHCD power consumption under DC or pulsed-DC inputs. In this regard, the presented model primarily assessed the elongated-trench MHCD power consumption under either DC or pulsed DC power during a stable mode of operation, which is a critical aspect to understanding the potential of the devices in fuel reforming applications. Furthermore, pulsed DC power is of particular interest for MHCDs as chemical reactors because it may improve reactant conversion while minimizing device electrode degradation [5,6,11]. The previously published MHCD circuit model studies did not simulate discharge current and voltage from pulsed-DC inputs, but we examined the current and voltage from pulsed-DC inputs in order to better understand the amplitude of the discharge current without current limiting. We assumed the circuit component values during stable operation remain valid for both DC and pulsed-DC inputs, since the simulated pulsed-DC inputs at 5–10 kHz had frequencies significantly slower than the relaxation oscillations of the Ar species in the plasma [48].

The microplasma inductance ("L_p, stable mode") was determined using the expression $L_p = R_p / v_m$ given by Chabert et al., where v_m represents an estimate for the electron-neutral collision frequency [42]. The value of the electron-neutral collision frequency, v_m, was $2.5 \ e^{-11} \ s^{-1}$ adopted from [42]. This electron-neutral collision frequency value for our particular device geometry with argon was verified according to the equation $v_m = N_{Ar_{neutral}} \sigma_{en} v_{te}$ [49]. In this equation v_m refers to the electron-neutral collision frequency, $N_{Ar_{neutral}}$ is the neutral argon density assuming the microplasma is weakly ionized with a degree of ionization less than 10% [50], σ_{en} is the electron-neutral collision cross section based on quantities from [51], and v_{te} is the electron thermal velocity assuming an electron temperature of 1 eV [3]. Checking the electron-neutral collision frequency under those parameters verified the electron-neutral collision frequency was the same order of magnitude as $2.5 \ e^{-11} \ s^{-1}$.

If a more complete treatment of the plasma resistance is integrated (i.e. not a single value) into the model an increase in plasma resistance would result in an increase in the microplasma inductance. In other words, when the plasma resistance increases to values that are indicative of an abnormal mode of operation, the resulting microplasma inductance, based on the expression $L_p = R_p / v_m$ would also increase and have a greater impact on the dynamics, especially if alternative types of power sources, like high frequency pulsed DC, were going to be simulated. However, as previously mentioned, we limited the model to only the stable mode of operation in which the plasma resistance is fixed to the value empirically determined that was observed during the stable mode of operation in order to compare the power consumption of the devices within the context of a fuel reforming application.

The capacitance, C, in Fig. 5 represents a microplasma capacitance. Both the vacuum capacitance of the device and sheath capacitances contribute to the microplasma capacitance, C, and thus it depends on the operating conditions of the MHCD elongated trench device. In order to estimate a value for that microplasma capacitance, C, the approach described in reference [41] was adopted. The estimated capacitance is identified as, C_{est}, and its physical meaning is the empirically determined microplasma capacitance based on the method described in [41]. The expression for C_{est} is $C_{est} = 1/(s(\Delta V))$, where s is the slope of the line relating experimentally collected data of the averaged self-pulsing current versus frequency [41]. The ΔV refers to the voltage variation during the observed self-pulsing regime given a specified MHCD device width. For the 25 μm wide MHCD with observed self-pulsing frequencies ranging from 28.7 to 270.1 Hz, the corresponding ΔV ranged from 100 to 110 V. For the 100 μm wide MHCD with

Fig. 5. Schematic of the electric circuit model developed for the MHCD device with an elongated trench during a stable operating mode for either pulsed DC or DC constant voltage inputs.

observed self-pulsing frequencies ranging from to 26.1 to 128.5 Hz, the corresponding ΔV ranged from 94 to 128 V. For the 250 μm wide MHCD with observed self-pulsing frequencies ranging from 236.4 Hz to 2363.4 Hz, the corresponding ΔV ranged from 44 to 86 V. In the model the numerical value of C corresponds to the value obtained for the 25 μm wide MHCD elongated trench device. The resulting numerical values for the electric circuit model of the MHCDs with elongated trenches are summarized in Table 1. The electric circuit model was implemented and simulated using MATLAB®'s Simscape™ software.

4. Results and discussion

4.1. Experimental results with constant voltage

During the experiments using a constant voltage source without current limitation, the current and voltage data collected from the MHCDs exhibited both self-pulsing and stable operating modes. The recorded self-pulsing current and voltage phenomena were used to estimate the microplasma capacitances. The recorded stable current and voltage data were used to estimate the microplasma resistance during stable operation. The following two sections further detail these experimental results.

4.1.1. Self-pulsing of the MHCDs with elongated trenches

The sharp transitions in the current data shown in Fig. 6(a) are indicative of an unstable, self-pulsing operating mode of our MHCD devices during constant voltage DC power application. Fig. 6(a) shows the current recorded for an MHCD with a trench 100 μm wide, a ballast resistance of 4.1 kOhm, and an Ar flow rate of 7.3 standard cm^3/min. The microplasma initiated at a voltage of 247 V, and was then maintained at 270 V for the duration of the experimental run.

The top plot in Fig. 6(a) is a time clip of one thousand seconds ($\sim$17 min). Fig. 6(a) further presents two additional views of a 110 s clip and a 5 s clip at the boxed temporal locations. In Fig. 6(a), there is an observable distribution of rates or frequencies of self-pulsing that occur with various current peaks. The pulsing seems to occur more rapidly in the beginning than the end of the experimental data collection.

The recorded self-pulsing electrical data were processed in order to determine estimates of the various self-pulsing frequencies and corresponding average current levels. The current had an average maximum of 32 mA and an average minimum near 0 mA. Fig. 6(b) shows the self-pulsing frequency versus averaged current calculated using seven data segments. The increasing linear trend in Fig. 6(b) verifies the existence of the capacitive element in the generated microplasma which is consistent with previous studies [26,35,39–42].

Self-pulsing under DC power application has been observed with other types of MHCD including cylindrical and micro-slit geometries [26,34,35,39–42]. The current data in Fig. 6(a) had slower pulses on the order of seconds in comparison to the self-pulses commonly reported for cylindrical MHCDs which are on
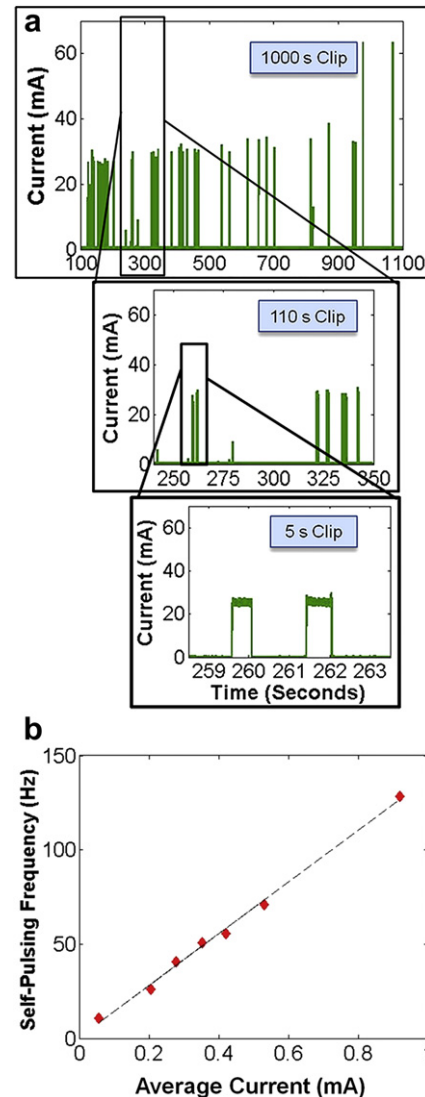
Table 1
Parameter values of elongated-trench MHCD circuit model.

Model parameter	Value or range	Units
DC input voltage	250–1000	V
Input pulse frequency	5–10	kHz
Ballast resistor, R_b	2.2	kOhm
Microplasma capacitance, C	70	μF
Microplasma resistance, R_p	100	kOhm
Microplasma inductance, L_p	0.4	μHenries

Fig. 6. (a) Self-pulsing current recorded from an MHCD with an elongated trench 100 μm wide for 270 V constant input voltage including temporally magnified views at the boxed locations. (b) Plot of self-pulsing frequency versus averaged current calculated using seven time-versus-current data segments from Fig. 6(a).

the order of milliseconds [35,39,41,42]. The self-pulsing signals from our devices had sharply defined waveforms like those reported by Aubert [26] and Rousseau [41] and more recently Chabert [42]. Analogous to these reports, the self-pulsing nature of our elongated-trench MHCD is believed to originate in the periodic extension of the microplasma outside the trench into the residual space volume above the chip. Previous studies indicated that observed increases in plasma volume likely emerge to sustain increased current levels at a given voltage [41,42]. Although there are analogous self-pulsing behaviors observed with the new elongated-trench MHCD devices likely due to similar phenomena without current limiting, further examination is required to understand the detailed nature of the physics behind self-pulsing states in the new devices given their trench geometry. The power supply voltage is the major factor observed to limit the microplasma self-pulsing discharge behaviors and presumably the plasma extension outside the trench [26,35,41]. A possible mechanism for preventing the self-pulsing is the addition of a cap or cover to seal the trench. Second generation, sealed MHCD devices

have been fabricated to investigate the impact of covering the trench in upcoming studies.

Additional experiments with MHCDs of varying channel width also exhibited self-pulsing behavior. For example, higher maximum self-pulsing rates were observed with devices 250 μm wide, a ballast resistance ranging from 2.2 to 3.9 kOhm and an Ar flow rate of 7.3 standard cm^3/min, when compared to the 100 μm wide device. From the self-pulsing current versus time data sets, the range of self-pulsing frequencies and associated average currents were determined. Fig. 7(a) shows the self-pulsing frequency versus average current data manifested during operation of the MHCD devices with widths of 25, 100 and 250 μm. For all of these experimental results, the constant voltage DC power supply was used with a series ballast resistance of 2.2 kOhm.

The slope of a line plotted in Fig. 7(a) is denoted by "s" in the expression, $C_{est}=1/(s(\Delta V))$ presented earlier in Section 3 [41]. The mean microplasma capacitances (C_{est}) for the 25, 100 and 250 μm wide devices were determined from the data shown in Fig. 7(a) with the intercepts set to zero and the corresponding measured ΔV. Fig. 7(b) summarizes the average estimated microplasma capacitances for the various channel widths. We found that all of the empirical microplasma capacitances were of the same order of magnitude. The 25 μm channel width had the largest standard error (defined as a function of both the standard error of the linear fit slope and the measured ΔV) whereas the 100 and 250 μm channel widths had smaller standard errors. The difference between the C_{est} for the 25 and 100 μm channel widths was insignificant, but the average C_{est} estimated for the 250 μm channel width was approximately half the value of the 25 and 100 μm widths' capacitances. Upon the tenfold increase in the microplasma channel width, and correspondingly the channel volume, the observed microplasma capacitance was effectively halved. The underlying principle that explains the observed difference in estimated capacitance for the 250 μm wide MHCD in comparison to the 25 or 100 μm wide devices is not clearly understood at this time, and requires further testing over a greater number of device widths between 25 and 250 μm.

The device capacitances without operating microplasmas, referred to as intrinsic capacitances, ranged from 620 pF for the 250 μm channel width to 650 pF for the 25 μm channel width. These values were calculated based on the expression for parallel plate capacitors. The estimated capacitances of the microplasmas present in the MHCD with elongated trenches were approximately five orders of magnitude larger than the intrinsic device capacitances of the devices with the equivalent geometry. This situation differs for cylindrical MHCDs in which the expressions for C_{est} and $C_{intrinsic}$ yielded values on the same order of magnitude of ≈ 100 pF [41]. The microplasma volumes of our elongated-trench devices ($V_{trench} \approx 0.0255-0.255$ mm^3) are one to two orders of magnitude greater than the microplasma volumes of the cylindrical devices ($V_{cylindrical} \approx 0.001$ mm^3), but the estimated capacitances for our trench devices are approximately five orders of magnitude larger than estimated capacitances for the cylindrical MHCDs. These findings indicate that microplasma volume is not related explicitly to the capacitance.

In addition to the observed self-pulsing, physical changes to the metal anode contacts were also observed as shown in Fig. 8. The changes to the electrode contacts resulted from phenomena such as material sputtering due to transient, intense, non-uniform microplasma exposure at localized anode locations and electromigration due to the high current densities (approximately on the order of 10^{10} A/m^2 without current limitation) [52,53]. Despite the physical changes to the interface between the trench and the anode contacts, our devices continuously operated during experimental runs of at least an hour under constant voltage without current-limiting capability. The full extent to which the physical changes to the anode contacts impacts the overall performance of our devices is another area for future examination. Pulsed-DC input power (discussed in Section 3 of the circuit model and Section 4.3) may help mitigate electrode degradation.

4.1.2. Normal mode operation of MHCDs with elongated trenches

In addition to the self-pulsing phenomena observed in MHCDs with elongated trenches, a stable, normal mode operation was also observed. Fig. 9 shows the voltage (solid line on the left vertical axis) and current (dashed line on the right vertical axis) recorded
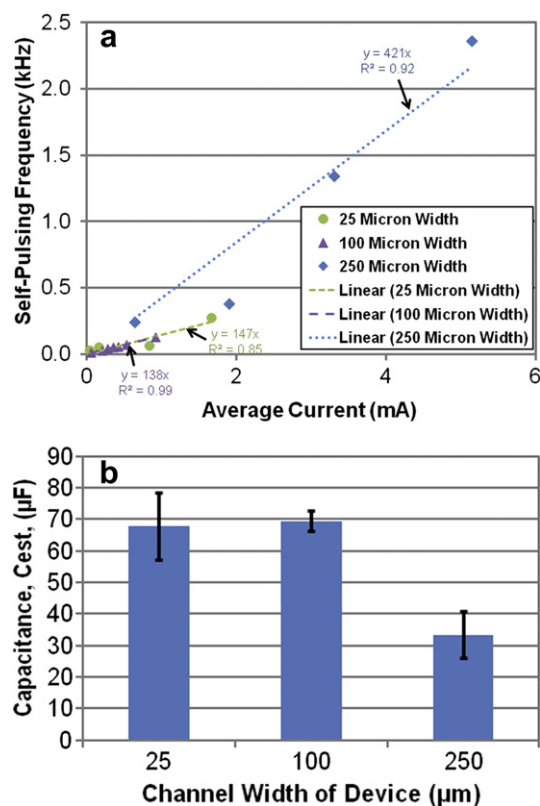

Fig. 7. (a) Self-pulsing frequency versus averaged current data manifested during operation of the MHCD devices with widths of 25, 100 and 250 μm. (b) Average estimated microplasma capacitances for the 25, 100 and 250 μm channel widths.
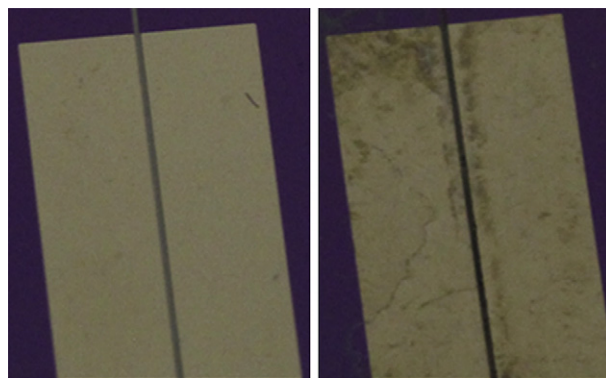

Fig. 8. Images of a 100 μm wide, elongated-trench MHCD before any microplasmas are initiated in the channel (left) in comparison to the 100 μm wide, elongated-trench MHCD used to collect the data from Fig. 6 after microplasma operation (right). The metal anode contacts have visible physical changes indicative of electrode degradation.
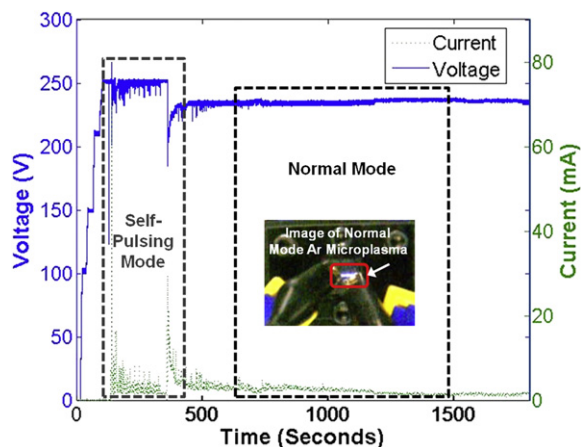
Fig. 9. Voltage (solid) and current (dotted) data recorded from a microplasma developed in an MHCD with an elongated trench 25 μm wide. An example of a microplasma that fills the entire trench length during normal mode operation is also presented.

from a microplasma developed in an MHCD with a trench 25 μm wide, a ballast resistance of 2.2 kOhm, and an Ar flow rate of 7.3 standard cm³/min. The inset photo shows normal mode operation of the microplasma with plasma filling the entire length of the elongated trench. The microplasma initiated at a voltage of 247 V. An input of 250 V was maintained from the high voltage DC power supply without current-limiting capability during the initial self-pulsing state of the MHCD and was then slightly lowered to 240 V for the remainder of the experimental run.

Fig. 9 shows that normal mode operation prevailed after an initial period of self-pulsing that immediately followed the microplasma onset. During normal mode operation, the voltage was steady at 237 V (±5 V), and the current, ranging from 1.5 to 3.5 mA, was low relative to the self-pulsing current values which exceeded 30 mA.

It is well established that the external circuitry connected to an MHCD device affects its operating mode [27]. The fact that a normal operating regime was observed suggests there are controllable operating states in which steady voltage and current can be achieved given the proper external circuitry. The existence of multiple operating modes, including self-pulsing, clearly indicates there are instabilities related to either transitions between modes [26,41] or characteristics arising from highly non-linear system dynamics [39,40]. Bearing in mind the intended application of microplasma reforming, it is advantageous to ensure a stable state for the MHCD devices with elongated trenches (such as normal mode) in order to optimize the efficiency of the device during use as a microplasma reformer, and ultimately ensure a steady outflow of hydrogen from a theoretically full-scale microplasma reforming system.

While increasing external resistance can dampen self-pulsing phenomena, the associated increased power dissipation motivates the pursuit of active external current-limiting, control circuitry. This is a particularly important consideration for use of the reported MHCD devices in hydrocarbon reforming applications in order to maximize the overall efficiency and minimize wasted energy [11,54]. Regardless of the specific approach pursued, limiting the current flowing through an MHCD device effectively curbs self-oscillation. Experiments conducted with a high voltage current-limited DC power supply are reported in the next section.

4.2. Experimental results with current-limiting

In order to test the MHCD under controlled current conditions, experiments with a high voltage, current-limited power supply (Stanford Research Systems, Inc.) were conducted. Fig. 10 shows the
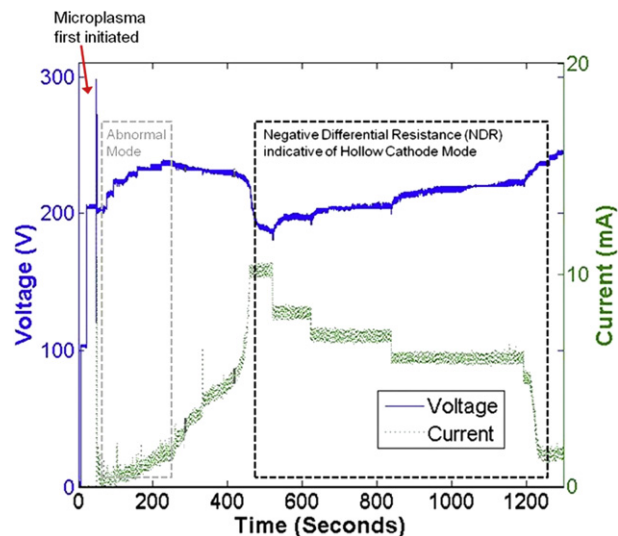

Fig. 10. Voltage (solid) and current (dotted) data recorded from a microplasma developed in an MHCD with an elongated trench 250 μm wide.

voltage given by the solid line on the left vertical axis and current given by the dashed line on the right vertical axis recorded from a microplasma developed in a trench 250 μm wide with a ballast resistance of 2.2 kOhm and an Ar flow rate of 7.3 standard cm³/min. The current limit on the power supply was initially set to 14 mA to facilitate microplasma initiation in the trench. The current was then manually adjusted to the values on the plot.

With the initially high current limit, the voltage was incrementally increased until the microplasma initiated. The current limit was then immediately reduced to 1 mA. In the first enclosed region, there was an abnormal mode of operation in which the voltage increased with increasing current. In the section with the decreasing current steps, the voltage and current data showed negative differential resistance (NDR) indicating a hollow cathode mode of operation. The slopes of the linear fits of the corresponding voltage versus current data estimated the plasma resistances for the hollow cathode or NDR mode ($R_{p, NDR}$) at approximately −7.5 kOhm.

Fig. 11(a) similarly shows a region of NDR. The voltage data given by the solid line on the left vertical axis and current data given by the dashed line on the right vertical axis in Fig. 11(a) were collected from an MHCD device 25 μm wide with a ballast resistance of 2.2 kOhm and an Ar flow rate of 7.3 standard cm³/min. Fig. 11(a) also includes an enlarged image of the MHCD being tested prior to the NDR region, providing an example of what the microplasma looked like when it filled the entire length of the trench. Fig. 11(b) plots the current versus voltage points for the 5 distinct current levels in Fig. 11(a), and also includes photos of the microplasmas in the trench corresponding to those points. The images clearly show a relationship between the current-limit in the NDR region and the extent to which the trench is filled. At the lowest current-limit the largest gap existed between microplasma regions, and became increasingly filled as the current-limit was increased. Once the trench is filled the device ceases to display NDR.

In both Figs. 10 and 11(a), self-pulsing voltage and current phenomena are not observed. This corroborates earlier findings that self-pulsing of the current and voltage in MHCDs is a function of plasma resistance, which strongly depends on the discharge current [26,35,39–42]. During constant voltage DC power application the maximum discharge current was able to exceed 30 mA and correspondingly had lower resistances during those peaks. A
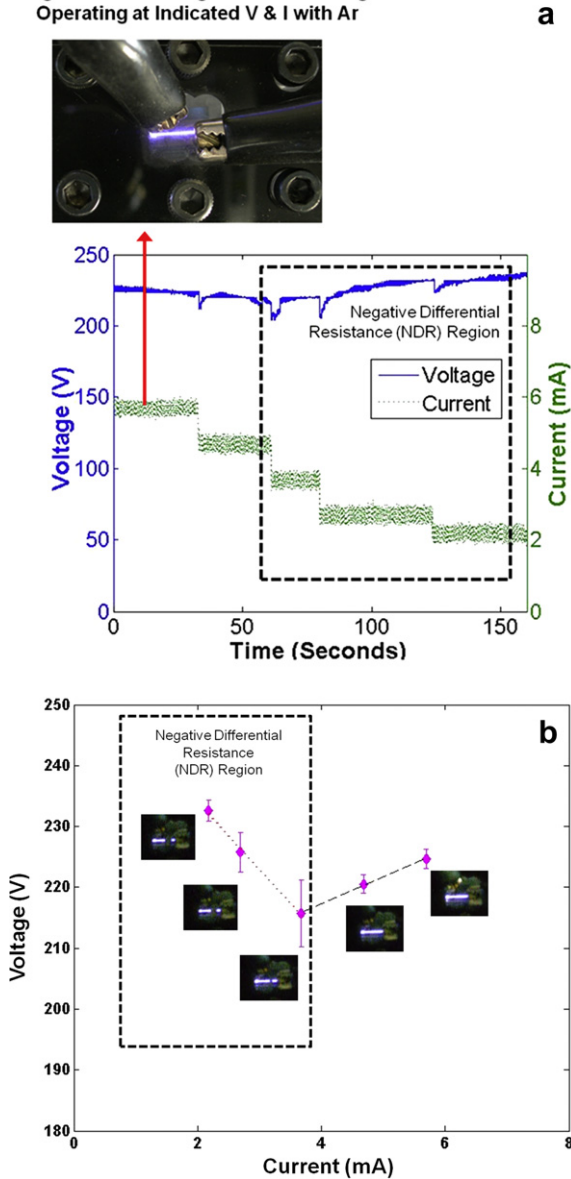
Fig. 11. (a) Voltage (solid) and current (dotted) data recorded from a microplasma developed in an MHCD with an elongated trench 25 μm wide including an image showing a microplasma that fills the entire trench length before stepping down the current and the onset of NDR. (b) Plot of the voltage versus current corresponding to the five distinct current levels presented in Fig. 11(a) including images of the microplasmas at those points. The data was collected by decreasing the current limit and taking the associated average voltage for each current step.

DC power source with current-limiting capability restricts the large amplitude current pulses (>30 mA) providing a means to prevent the abrupt transitions between MHCD operating modes, which otherwise result in the periodic expansion of the microplasma outside the trench causing self-pulsing.

The electrical data collected during current-limited DC power application exhibited clear regimes of NDR in which the voltage decreased with increased current. The NDR observed was related to the extent the microplasma filled the trench, and strongly depended on the current permitted to flow through the MHCD device. Since the microplasmas do not fill the entire length of the MHCD under certain conditions, the total microplasma capacitance would also vary as a function of the fraction of the channel filled.

As described in Section 3 on the electric circuit models of MHCD devices, theory regarding the mechanisms contributing to self-pulsing during DC power application varies [39–42]. Hsu and Graves held that the self-pulsing could be from instabilities due to NDR [39]. Fig. 11(a) and (b) showed with current-limiting, NDR was observed but without the incidence of microplasma self-pulsing. Rousseau, Aubert, and most recently Chabert extended Hsu and Graves' investigation on MHCD self-pulsing, and attributed the self-pulsing to switching or transitioning between specific operating modes of MHCD devices [41,42]. Based on this explanation for self-pulsing during DC power, Rousseau and Aubert further developed an expression to estimate the microplasma capacitance which we applied in this study [41]. When our devices were self-pulsing, the microplasma filled the entire trench during their "on" states, and resembled the images in Fig. 11(b) for currents greater than 4.5 mA. Therefore the microplasma capacitances empirically determined in this study apply when the microplasma extends the full length of the trench. The application of current-controlled DC power prevented self-pulsing, enabled the observation of distinct operating modes based on the current-limit setting and associated voltage levels, and improved operating control of our MHCDs.

4.3. Power consumption of the MHCD devices based on the circuit model

Since findings suggest that pulsed DC power may facilitate chemical conversion within microplasma reactors [3,6,11] we modeled the total power consumption of the elongated-trench MHCDs for both DC and pulsed-DC inputs. The circuit model given in Fig. 5 and run in this study used a normal mode plasma resistance derived from empirical current and voltage data. Table 2 summarizes the total power consumption values that were obtained in the simulations.

A DC input of 250 V was simulated for the electric circuit model as the basis of comparison for the power consumption with the pulsed DC voltage inputs. For the reference DC input, which is the same as the input used to obtain the voltage and current data in

Table 2
Summary of the MHCD electric circuit simulation runs.

Input voltage parameters				Total current (mA)	MHCD voltage (V)	Average power (W) based on provided expression for pulsed inputs		
Type	Amplitude (V)	Frequency (kHz)	Width (% of period)	$I_t = I_1 + I$ RMS for pulsed inputs	V_{MHCD} RMS for pulsed inputs	Total: $P_{avg} = \frac{1}{T} \int v_{in}(t) i_{total}(t) dt$	R_p: $P_{avg} = \frac{1}{T} \int v_{MHCD}(t) i(t) dt$	R_b: $P_{avg} = I_{t,rms}^2 R_b$
DC	250	NA	NA	2.4	245	*00.61*	*00.60*	00.01
Pulsed	250	5	50	57.9	116	*7.77*	*0.13*	7.38
Pulsed	500	5	50	115.8	231	*31.08*	*0.54*	29.52
Pulsed	250	10	25	50.0	59	*5.61*	*0.04*	5.50
Pulsed	500	10	25	100.0	118	*22.42*	*0.14*	22.01

The values have been italicised in order to to maintain consistency with the format of the parameters as they were presented in the text of section 3

Fig. 9 for a 25 μm wide MHCD, the total power entering the ballast resistor and device was less than 1 W. Our MHCDs typically required less than 2 W of power over the experimental range of DC voltages explored using Ar. In contrast the total average input power resulting from the pulsed-DC input signals detailed in Table 2 were higher and ranged from 5.61 to 31.08 W. Although a pulsed supply may improve reaction yield [3,6,11] the higher average power consumption could offset this potential benefit, which is particularly relevant for portable reforming applications.

5. Conclusions and recommendations

MHCD devices with elongated, microfabricated trenches oriented in the lateral direction to facilitate reactant gas flow were electrically characterized and modeled. Self-pulsing, similar to that reported for other MHCD geometries, was observed during constant voltage DC power application. Using the self-pulsing current data the capacitances of the atmospheric pressure Ar microplasmas were estimated to be on the order of microfarads (μF), approximately five orders of magnitude larger than those reported for cylindrical MHCDs.

The observed self-pulsing phenomena indicated the presence of an unstable operating mode which could lead to inconsistent generation of products in the context of chemical reaction applications. This is a key challenge to implementing these devices as compact microplasma reformers for generating H_2 from hydrocarbons. However, intentional pulsing of the MHCD is not objectionable *per se* based on the prospect of higher electron densities, but robust control of the device is imperative for steady operation. As demonstrated in our experiments simple current-limiting resulted in steady operation. In an actual microplasma reforming system, a control mechanism with this as its basis could be employed.

Other operating modes observed during current-limited DC power application included abnormal, normal, and hollow cathode (NDR) modes of operation. The NDR operating mode was strongly dependent on the current limit, which in turn influenced the extent to which the microplasma filled the trench. This finding implies that a specific minimum current-level exists (for a given input gas composition) in which microplasma fills the entire trench offering a maximum volume for reaction.

The empirical circuit model developed from the electrical characterization of our devices gave the simulated average power consumption with DC and pulsed supplies during a stable, normal mode of operation. Higher average power consumptions were obtained under pulsed DC power, but pulsed DC also offers the prospective benefits of enhanced electron densities and reduced electrode degradation. The presented model was limited to simulation of the devices during a normal, stable mode of operation. To extend the model's capability to simulate additional operating states, future work is recommended to incorporate a dynamic expression for the plasma resistance as a function of the current, similar to the approach described in Chabert et al. [42].

Physical changes to the electrode contacts were clearly observed in our experiments. The potential benefits of pulsed DC power application must be more rigorously examined in light of the larger average power consumption, especially in the reforming application, where the energy expenditure is critical. A recent investigation of methane chemical conversion within the elongated-trench MHCD during DC versus pulsed DC power has been reported by Besser and Lindner [11]. Additional studies are recommended to compare the chemical conversion within the elongated-trench MHCD during DC versus pulsed DC power using a variety of hydrocarbon feeds. Follow-on studies are also recommended to better understand the mechanisms behind the physical changes to the electrodes of this novel MHCD with DC versus pulsed DC power.

References

[1] K.H. Becker, K.H. Schoenbach, J.G. Eden, J. Phys. D: Appl. Phys. 39 (2006) R55.
[2] C. Penache, M. Miclea, A. Bräuning-Demian, O. Hohn, S. Schössler, T. Jahnke, K. Niemax, H. Schmidt-Böcking, Plasma Sources Sci. Technol. 11 (2002) 476–483.
[3] M. Moselhy, I. Petzenhauser, K. Frank, K.H. Schoenbach, J. Phys. D: Appl. Phys. 36 (2003) 2922–2927.
[4] X. Guangqing, M. Genwang, N. Sadeghi, Tsinghua Sci. Technol. 14 (2009) 49–53.
[5] R. Foest, M. Schmidt, K. Becker, Int. J. Mass Spectrom. 248 (2006) 87–102.
[6] H. Qui, K. Martus, W.Y. Lee, K. Becker, Int. J. Mass Spectrom. 233 (2004) 19–24.
[7] T. Nozaki, A. Hattori, K. Okazaki, Catal. Today 98 (2004) 607–616.
[8] P. Sichler, S. Büttgenbach, L. Baars-Hibbe, C. Schrader, K.-H. Gericke, Chem. Eng. J. 101 (2004) 465–468.
[9] A. Koutsospyros, S.-M. Yin, C. Christodoulatos, K. Becker, Int. J. Mass Spectrom. 233 (2004) 305–315.
[10] P.J. Ricatto, V. Deligiannakis, J. Hunt, H. Ghezel-Ayagh, D. Dietz, C. Christodoulatos, K. Becker, Proceedings 3rd International Workshop on Microplasmas (2006) Greifswald, Germany.
[11] R.S. Besser, P.J. Lindner, Microplasma reforming of hydrocarbons for fuel cell power, J. Power Sources 196 (2011) 9008–9012.
[12] A. Indarto, N. Coowantiwong, J. Choi, H. Lee, H. Song, Fuel Process. Technol. 89 (2008) 214–219.
[13] E. Stoffels, I.E. Kieft, R.E.J. Sladek, J. Phys. D: Appl. Phys. 36 (2003) 2908–2913.
[14] J.A. Pérez-Martínez, R. Peña-Eguiluz, R. López-Callejas, A. Mercado-Cabrera, R.A. Valencia, S.R. Barocio, J.S. Benítez-Read, J.O. Pacheco-Sotelo, Surf. Coat. Technol. 201 (2007) 5684–5687.
[15] M. Moreau, N. Orange, M.G.J. Feuilloley, Biotechnol. Adv. 26 (2008) 610–617.
[16] G.E. Morfill, M.G. Kong, J.L. Zimmermann, New J. Phys. 11 (2009) 115011.
[17] B. Gweon, D.B. Kim, S.Y. Moon, W. Choe, Curr. Appl. Phys. 9 (2009) 625–628.
[18] S. Deng, C. Cheng, G. Ni, Y. Meng, H. Chen, Curr. Appl. Phys. 10 (2010) 1164–1168.
[19] P.S. Kothnur, L.L. Raja, Contrib. Plasma Phys. 47 (2007) 9–18.
[20] K.H. Schoenbach, A. El-Habachi, W. Shi, M. Ciocca, Plasma Sources Sci. Technol. 6 (1997) 468–477.
[21] A. El-Habachi, M. Moselhy, A. El-Dakroury, K.H. Schoenbach, Plasma Science, ICOPS' 99. IEEE Conference Record − Abstracts (1999).
[22] D.-L. Biborosch, E. Uwe, P. Gheorghe, F. Klaus, J. Plasma Fusion Res. 4 (2001) 297–300.
[23] J. Chen, S.-J. Park, Z. Fan, J.G. Eden, C. Liu, J. Microelectromech. Syst. 11 (2002) 536–543.
[24] G.J. Kim, Y.J. Hong, F. Iza, J.K. Lee, Comput. Phys. Commun. 177 (2007) 131.
[25] X.W. Gu, L. Meng, Y. Yan, Y.Q. Sun, Contrib. Plasma Phys. 49 (2009) 40–48.
[26] X. Aubert, G. Bauville, J. Guillon, B. Lacour, V. Puech, A. Rousseau, Plasma Sources Sci. Technol. 16 (2007) 23–32.
[27] D. Staack, B. Farouk, A. Gustol, A. Fridman, Plasma Sources Sci. Technol. 14 (2005) 700–711.
[28] C. Lazzaroni, P. Chabert, A. Rousseau, N. Sadeghi, J. Phys. D: Appl. Phys. 43 (2010) 124008.
[29] K.H. Schoenbach, M. Moselhy, W. Shi, Plasma Sources Sci. Technol. 13 (2004) 177–185.
[30] P.S. Kothnur, L.L. Raja, J. Appl. Phys. 97 (2005) 043305.
[31] T. Farouk, B. Farouk, D. Staack, A. Gustol, A. Fridman, Plasma Sources Sci. Technol. 15 (2006) 676–688.
[32] T. Farouk, B. Farouk, D. Staack, A. Gustol, A. Fridman, Plasma Sources Sci. Technol. 16 (2007) 619–634.
[33] N. Takano, K.H. Schoenbach, Plasma Sources Sci. Technol. 15 (2006) S109–S117.
[34] W. Zhu, N. Takano, K.H. Schoenbach, D. Guru, J. Mclaren, J. Heberlein, R. May, J.R. Cooper, J. Phys. D: Appl. Phys. 40 (2007) 3896–3906.
[35] T. Deconinck, L.L. Raja, Plasma Processes Polym. 6 (2009) 335–346.
[36] T.I. Farouk, Modeling and Simulations of DC and RF Atmospheric Pressure Non-Thermal Microplasma Discharges: Analysis and Applications, Drexel University, Philadelphia, PA, USA, 2009.

[37] K.H. Schoenbach, R. Verhappen, T. Tessnow, F.E. Peterkin, Appl. Phys. Lett. 68 (1996) 13–15.
[38] F. Adler, E. Davliatchine, E. Kindel, J. Phys. D: Appl. Phys. 35 (2002) 2291–2297.
[39] D.D. Hsu, D.B. Graves, J. Phys. D: Appl. Phys. 36 (2003) 2898–2907.
[40] D. Staack, B. Farouk, A. Gustol, A. Fridman, J. Appl. Phys. 106 (2009) 013303.
[41] A. Rousseau, X. Aubert, J. Phys. D: Appl. Phys. 39 (2006) 1619–1622.
[42] P. Chabert, C. Lazzaroni, A. Rousseau, J. Appl. Phys. 108 (2010) 113307.
[43] U. Kogelschatz, Contrib. Plasma Phys. 47 (2007) 80–88.
[44] D.D. Hsu, D.B. Graves, Plasma Chem. Plasma Process 25 (2005).
[45] K. Shah, R.S. Besser, J. Power Sources 166 (2007) 177–193.
[46] E. Lennon, A.A. Burke, M. Ocampo, R.S. Besser, J. Power Sources 195 (2010) 299–306.
[47] H. Surangalikar, X. Ouyang, R.S. Besser, Chem. Eng. J. 93 (2003) 217–224.
[48] S. Tajima, M. Matsumori, S. Nakatsuka, S. Tsuchiya, T. Ichiki, J. Appl. Phys. 108 (2010) 083302.
[49] R.L. Merlino, N. D'Angelo, Phys. Plasmas 12 (2005) 054504.
[50] L.G. Christophorou, J.K. Olthoff, Fundamental Electron Interactions with Plasma Processing Gases, Kluwer Academic/Plenum Publishers, New York, NY USA, 2004.
[51] http://jila.colorado.edu/~avp/collision_data/electronneutral/hayashi.txt August 24, 2011.
[52] M. Braunovic, N.K. Myshkin, V.V. Konchits, Electrical Contacts Fundamentals, Applications and Technology, CRC Press, Boca Raton, FL USA, 2007.
[53] T.H. Tran, S.J. You, M. Park, J.H. Kim, D.J. Seong, Y.H. Shin, J.R. Jeong, Atmospheric pressure microplasma source based on parallel stripline resonator, Curr. Appl. Phys. 11 (2011) S126–S130.
[54] W.B. Zimmerman, Chem. Eng. Sci. 66 (2011) 1412–1425.